Geodynamic Significance of the Kontum Massif in Central Vietnam: Composite $^{40}Ar/^{39}Ar$ and U-Pb Ages from Paleozoic to Triassic

Elizabeth A. Nagy,[1] *Henri Maluski,*[2] *Claude Lepvrier,*[3] *Urs Schärer, Phan Truong Thi,*[4] *A. Leyreloup,*[2] *and Vu Van Thich*[2]

Laboratoire de Géochronologie, Université Paris 7 and Institute de Physique du Globe de Paris, 2 Place Jussieu, F-75251 Paris Cedex 05, France (e-mail: eanagy@syr.edu)

ABSTRACT

The Kontum massif of south-central Vietnam has long been classified as lower continental crust of Precambrian (Archean) age. U-Pb zircon and $^{40}Ar/^{39}Ar$ biotite ages from charnockites and amphibolite facies rocks from this basement, however, yield much younger ages and imply at least two Paleozoic thermal events. Syntectonic charnockites from the Kannack complex and the southern Kontum massif record Permo-Triassic magmatism (U-Pb: 249 ± 2[2σ] Ma and 253 ± 2 Ma). The former sample yields an $^{40}Ar/^{39}Ar$ age of 243 ± 4 Ma (2σ), implying rapid cooling to the 250°C isograd following emplacement into the lower crust. The ages confirm the importance of Permo-Triassic magma-generating orogenesis throughout a large part of eastern Indochina probably related to the closing of the Paleo-Tethys Sea. Older ages in amphibolite facies igneous and metamorphic rocks from the western Kontum massif record magmatic emplacement at 451 ± 3 Ma (U-Pb) and possibly a Paleozoic tectonometamorphic event (~340 Ma) that partially to completely reset the argon systems ($^{40}Ar/^{39}Ar$: 424 ± 5 Ma, 380 ± 3 Ma, and 339 ± 4 Ma). Crustal thickening and regional heating during suturing of the Indochina block to the South China block along the Song Ma suture zone may have produced the 340 Ma low-temperature thermal event, although slow variable cooling could also explain the argon data. The Kontum massif and Kannack metamorphic complex should henceforth be considered exposures of deep crustal levels of the Permo-Triassic orogeny in contact with Paleozoic midcrustal rocks. Evidently, the Kontum massif did not rift from a Precambrian granulite belt in Gondwana.

Introduction

Granulite and amphibolite facies metamorphic rocks of the Kontum massif in central Vietnam have traditionally been interpreted as an uplifted Precambrian (Archean) fragment of continental crust that rifted from Gondwana and subsequently represented the core of the Indochina block in paleogeographic reconstructions of southeast Asia (e.g., Metcalfe 1988, 1996, 1999; Hutchison 1989; Sengör and Natal'in 1996). The Kontum craton is consequently taken as evidence for Precambrian/early Paleozoic geologic events, such as magmatism associated with Neo-Proterozoic collisions (e.g., Sengör et al. 1988; Sengör and Natal'in 1996). On the basis of petrologic similarities with rock assemblages in East Antarctica, India, Sri Lanka, and Australia, the granulite facies formations of the Kontum massif have also been considered the missing piece that fills a gap between these other elements of a major Precambrian granulite belt (e.g., Katz 1993).

Only a handful of the magmatic and metamorphic rocks from inferred Precambrian basement in Vietnam have been dated and reported with procedural details and supporting analytical data. Exposures of possible Precambrian basement within Vietnam are limited to the Kontum massif, the Bu Khang area, and along the Red River fault zone (fig.

Manuscript received October 10, 2000; accepted April 24, 2001.

[1] Present address: Department of Earth Sciences, Syracuse University, Syracuse, New York 13244-1070, U.S.A.

[2] Centre National de la Recherche Scientifique-ISTEM-Université Montpellier 2, Place Eugène Bataillon, 34095 Montpellier, France.

[3] Laboratoire de Tectonique, ESA-Centre National de la Recherche Scientifique 7072, case 129-t 26-E1, Université Pierre et Marie Curie, 4 Place Jussieu, 75252 Paris Cedex 05, France.

[4] National University of Vietnam, Hanoi, 334 Nguyen Trai Street, Thanh Xuan, Hanoi, Vietnam.

[The Journal of Geology, 2001, volume 109, p. 755–770] 0022-1376/2001/10906-0005$01.00

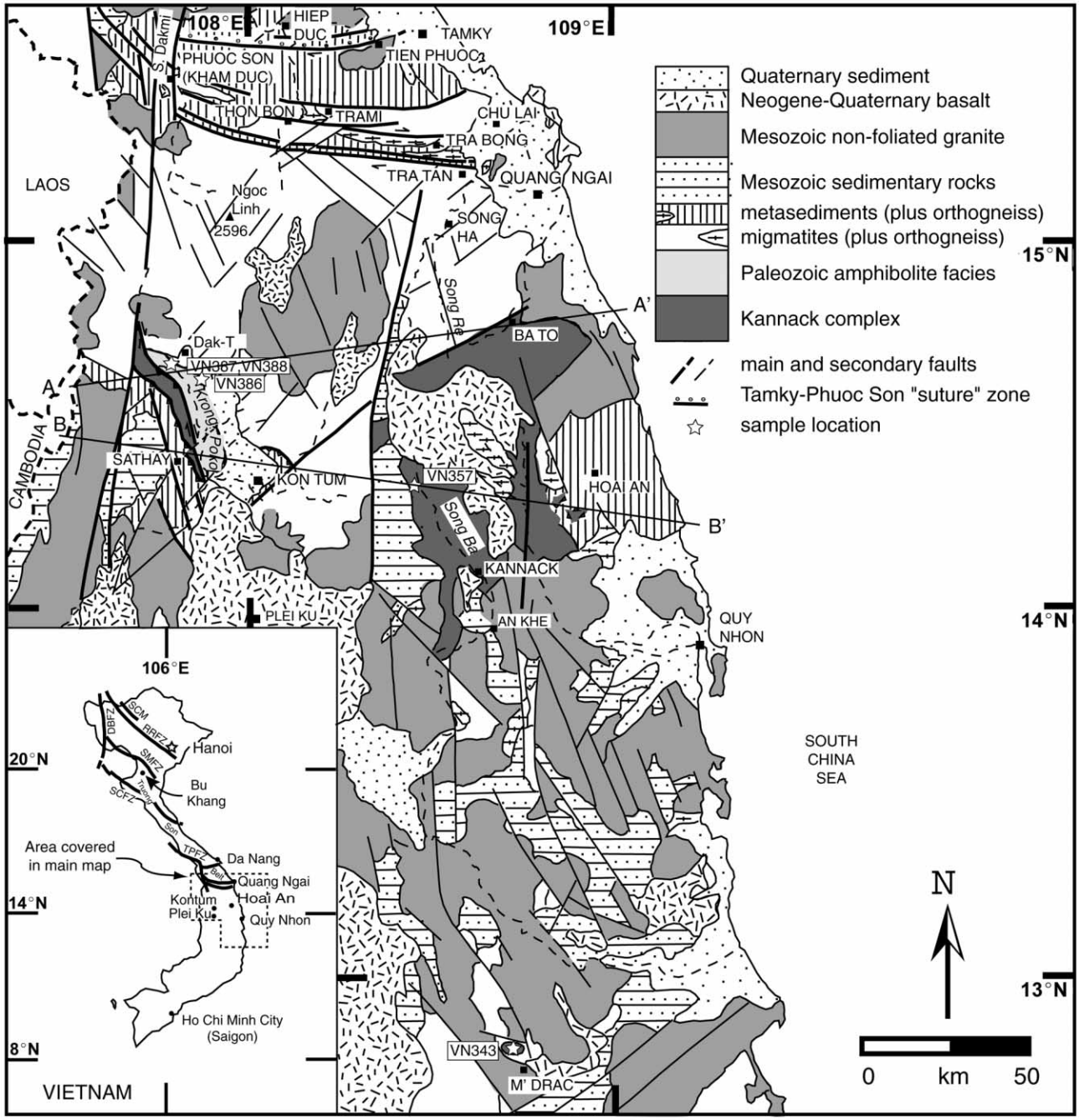

Figure 1. Simplified geologic map of the Kontum massif in Vietnam showing sampling sites and regions discussed in text. Map is compiled from existing geologic maps and present field investigations. Map units are after Tran Van Tri (1973) and Nguyen Xuan Bao et al. (1994). Heavy dashed lines are international borders; light dashed lines are rivers. The Kannack complex consists of granulite facies rocks and syntectonic charnockite intrusions. The Paleozoic amphibolite facies rocks include acidic to basic orthogneisses known as the Dak-Tô Unit. Undated amphibolite facies rocks, which include migmatitic gneisses, orthogneisses, and metasediments, are the Ngoc Linh complex and the Kham Duc formation. Mesozoic terrigenous sediments are Triassic and Jurassic. *Inset*, Map of Vietnam showing major fault zones, cities, and towns mentioned in the text and the location of the main geologic map. *DBFZ* = Dien Bien Phu fault zone; *RRFZ* = Red River fault zone; *SCM* = Song Chay massif; *SCFZ* = Song Ca fault zone; *SMFZ* = Song Ma fault zone; *TPFZ* = Tamky–Phuoc Son fault zone.

1, inset). Early Proterozoic K-Ar ages of 1.7–2.0 Ga (Tran Ngoc Nam 1998), as well as Nd model ages of 3.4–3.1 Ga (Lan et al. 1999), have been documented along the Red River fault zone, although single-grain U-Pb-Hf isotope analyses from detrital zircon and baddeleyite crystals from the Red River are not in favor of crust older than 2.5 Ga along this major drainage (Bodet and Schärer 2000). Inherited zircon components corroborate melting of Precambrian (1.6–0.8 Ga) crust in Oligo-Miocene gneisses from the Red River and Bu Khang areas (Schärer et al. 1990, 1994; Nagy et al. 1999, 2000), although direct evidence for Precambrian rocks has not been reported from the Bu Khang region. Ages from the Kontum massif include a few early to middle Proterozoic K/Ar and Rb-Sr ages, as well as a Cambrian Rb-Sr age and a Devonian K/Ar age, although analytical details are missing from many of these early studies (Faure and Fontaine 1969; Snelling 1969; Hurley and Fairbairn 1972; Phan Truong Thi 1985; Tran Quoc Hai 1986; Hutchison 1989). Recent geochronologic studies in the Kontum massif find Nd model ages of 2.0–1.5 Ga (Lan et al. 2000) and SHRIMP U-Pb zircon ages from one granulite sample of 254 Ma (Tran Ngoc Nam et al. 2001).

We present the first $^{40}Ar/^{39}Ar$ and U-Pb combined geochronologic results for a variety of rocks from the Kontum basement, including the Kannack metamorphic complex, and show that these rocks do not represent Precambrian lower crust but rather record Paleozoic to Triassic magmatism and low-temperature thermal events. Our results have important implications for the extent of magmatism related to the late Paleozoic closing of the Paleo-Tethys Sea.

Geologic Setting and Sample Locations

The Kontum massif (Saurin 1944) in south-central Vietnam is an uplifted block of high-grade metamorphic rocks intruded by granitic bodies and largely covered by Neogene-Quaternary basalts (Rangin et al. 1995; Hoang and Flower 1998; Lee et al. 1998). The E-to-W-striking Tamky–Phuoc Son fault zone (fig. 1 and inset) separates the Kontum block from the Truong Son fold belt to the north. The Truong Son belt, which strikes ~NW and extends from central Vietnam through north-central Vietnam and into northeastern Laos, consists primarily of elongated zones of metamorphic rocks. The Song Ca and Song Ma fault zones (fig. 1, inset) are 250–300-km-long continuous shear zones within the Truong Son belt that show metamorphic fabrics parallel to the overall trend of the range (e.g., Lepvrier et al. 1997).

South of the Tamky–Phuoc Son fault zone, the supposedly Precambrian Kannack metamorphic core complex, located primarily in the east-central part of the Kontum block with smaller isolated exposures in the south near M'Drac and in the west near Dak-Tô (fig. 1), is intruded by Paleozoic and undated amphibolite facies rocks and by Mesozoic nonfoliated granites. Mesozoic sediments are present as well. All of these rocks have been extensively faulted by structures generally striking N to NNW, whereas Neogene-Quaternary basalts and sediments in the region are not deformed by brittle deformation.

The Kannack metamorphic complex includes several formations preserving granulite facies rock types (DGMVN 1997). All rocks in the complex are related to the 2-pyroxene gneiss facies of regional metamorphism (Hutchison 1989), corresponding to conditions of formation at deep crustal levels around 800°–850°C and 7–8 kbar (Tran Quoc Hai 1986). The base of the complex is formed by an aluminous metasedimentary series (pelites and Al-quartzites) intercalated with carbonate (more or less dolomitic) sediments. These undated sedimentary protoliths are highly foliated (sometimes mylonitic) and metamorphosed to granulite facies, giving rise to khondalitic and kinzigitic gneisses, granulitic metaquartzites, marbles, and skarns. The foliation is flat to moderately dipping. Intermediate pressures are supported by prismatic biotite and sillimanite-garnet-K-feldspar mineralogy. Prismatic rutile, Mg-ilmenite, Ti-magnetite, sulfur, apatite, zircon, and graphite are abundant. The presence of stable biotite with quartz in some samples indicates that anatectic conditions, probably under low pH_2O, were attained.

Syntectonic bodies of charnockite intrude the granulitic metasedimentary formation. Evidence for the syntectonic nature of the intrusions includes magmatic foliation that parallels the foliation of the granulites and foliation-parallel intrusions of large sills. Most of the charnockites belong to either a calc-alkaline magmatic series or a continental tholeiitic series with plagioclase and orthopyroxene. The magmatic suite is differentiated into acidic, intermediate, and basic members, giving rise to charno-enderbites, Q-enderbites with orthopyroxene and biotite (Phan Cu Tien et al. 1988), and true noritic gabbros. The most acidic charnockitic rocks could be products of anatexis of the granulitic metasediments under low pH_2O conditions. The charnockites and granulites display a late (secondary), retrograde greenschist facies metamorphism (e.g., chloritization of biotite, Fe loss in biotites, growth of opaques and secondary white-

micas). Cordierite may be pinitized and brown hornblende can be transformed into actinolite and epidote. This retrogressive episode may simply be due to cooling of the syntectonic magmas or it may have formed as the result of independent, late, low-grade metamorphism. Our study includes a Q-enderbite charnockite (VN357) analyzed with U-Pb, Rb-Sr, and $^{40}Ar/^{39}Ar$ methods (14°15′45″; 108°30′17″).

North and south of the Kannack complex, large amounts of migmatitic gneisses and strongly foliated granites are exposed. These rocks display a N-to-NE-striking foliation and a general antiformal structure (see cross sections in fig. 2). Shear criteria across the area indicate normal movements related to exhumation of the massif. The direction of extension is approximately NW to SE. The mineral assemblage corresponds to amphibolite facies with muscovite and sillimanite. In contrast to the Kannack complex, migmatization occurs in the presence of water. We have analyzed a charnockite (Q-enderbite) enclave (VN343) from within this unit from the southernmost part of the Kontum massif (fig. 1) with the U-Pb and Rb-Sr methods (12°46′47″; 108°40′50″).

In the western part of the Kontum block, a NNW-trending zone along the Krong Poko River between the villages of Dak-Tô and Kontum (fig. 1) consists of amphibolites and granitoids more or less gneissified (Phan Cu Tien et al. 1988). To the west, these rocks are in fault contact over a slice of Kannack complex rocks; Neogene sediments cover the eastern contact. The rocks do not share any features with the previously described charnockites, and from a geochemical point of view, they belong to a Fe-K-rich series. We sampled three different amphibolite facies metabasites representing alkaline to calc-alkaline affinities. Sampled outcrops consist of a N110°E-to-N160°E-striking, subvertical foliation and subhorizontal lineations. A biotite-enriched pelitic series within the orthogneiss expresses strong foliation and isoclinal folding. Shear criteria tend to indicate a dextral sense of motion. Our samples include a weakly deformed granodiorite (VN386; 14°36′49″; 107°51′31″), an orthogneiss (VN387; 14°39′06″; 107°47′20″), and a biotite amphibolite (VN388; same location as VN387). We analyzed sample VN386 with U-Pb and Rb-Sr methods and all three samples for $^{40}Ar/^{39}Ar$.

Mineralogy and Geochemistry

Charnockites. Sample VN357 is a Q-enderbite that is typical of intermediate-to-acidic units found in the Kannack complex. It contains quartz, andesine plagioclase ($An_{0.40-0.43}Ab_{0.54-0.57}Or_{0.03-0.04}$) containing antiperthetic K-feldspar ($Ab_{0.05}Or_{0.95}$), myrmekitic K-feldspar, hypersthene ($Fe_{0.39}$), Ti-biotite, Ti-hornblende, apatite, zircon, and Ti opaques. (All phenocryst compositions quoted here were determined with a Cameca SX 100-5 electron microprobe at the University of Montpellier 2.) The biotite occurs as a syn- to late-crystallization phase, formed after the initial crystallization of orthopyroxene, and brown hornblende crystallized even later.

Sample VN343 is a Q-enderbite occurring within migmatites and consists of quartz, metastable ceriticized plagioclase exhibiting polysynthetic twinning, myrmekitic K-feldspar, orthopyroxene, chloritized biotite, muscovite, secondary amphibole, apatite, and zircon. There is evidence for both primary and secondary muscovite. The petrofabric indicates brittle deformation.

Amphibolite Facies Rocks. Sample VN386 is a weakly foliated granodiorite containing quartz, K-feldspar, oligoclase plagioclase, Fe/Ti-biotite, and zircon. Sample VN387 is an orthogneiss consisting of quartz, K-feldspar, oligoclase plagioclase, Fe/Ti-biotite, Fe-hornblende, allanite, titanite, apatite, zircon, and opaques. Finally, VN388 is a biotite amphibolite of dioritic composition, consisting of quartz, andesine plagioclase ($An_{0.39}$), green-brown amphibole (Fe-pargasite/hastingsite with $Fe_{0.52-0.59}$; 0.9–1.13 wt % TiO_2), Fe/Ti biotite ($Fe_{0.56}$; 2.65 wt % TiO_2), epidote (var. pistacite), titanite, allanite, ilmenite, apatite, and zircon.

Geochemistry. Chemical analyses of powdered whole rock splits from the three samples analyzed for U-Pb and Rb-Sr (charnockites VN357 and VN343 and granodiorite VN386) were performed using emission-ICP for major element determinations and ICP-MS for trace and rare earth element (REE) analyses (table 1 [tables 1, 3, and 5 are available from *The Journal of Geology* Data Depository free of charge upon request]). Rock classification for each sample is assigned using a silica-alkali diagram (fig. 3*a*). Major and trace element data show that the three intrusions reflect calc-alkaline magmas lying in the fields of diorite (VN357), granodiorite (VN386), and granite (VN343). All samples are LREE (light rare earth element) enriched with La/Yb > 10 (fig. 3*b*). Charnockite VN357 is the least fractionated of the three samples, and charnockite VN343 is the most fractionated and significantly depleted in HREE (heavy rare earth element) (La/Yb = 48), suggesting garnet fractionation in the source magma. Eu anomalies are slightly negative (VN357) to absent; plagioclase fractionation is therefore not strongly supported. In trace element

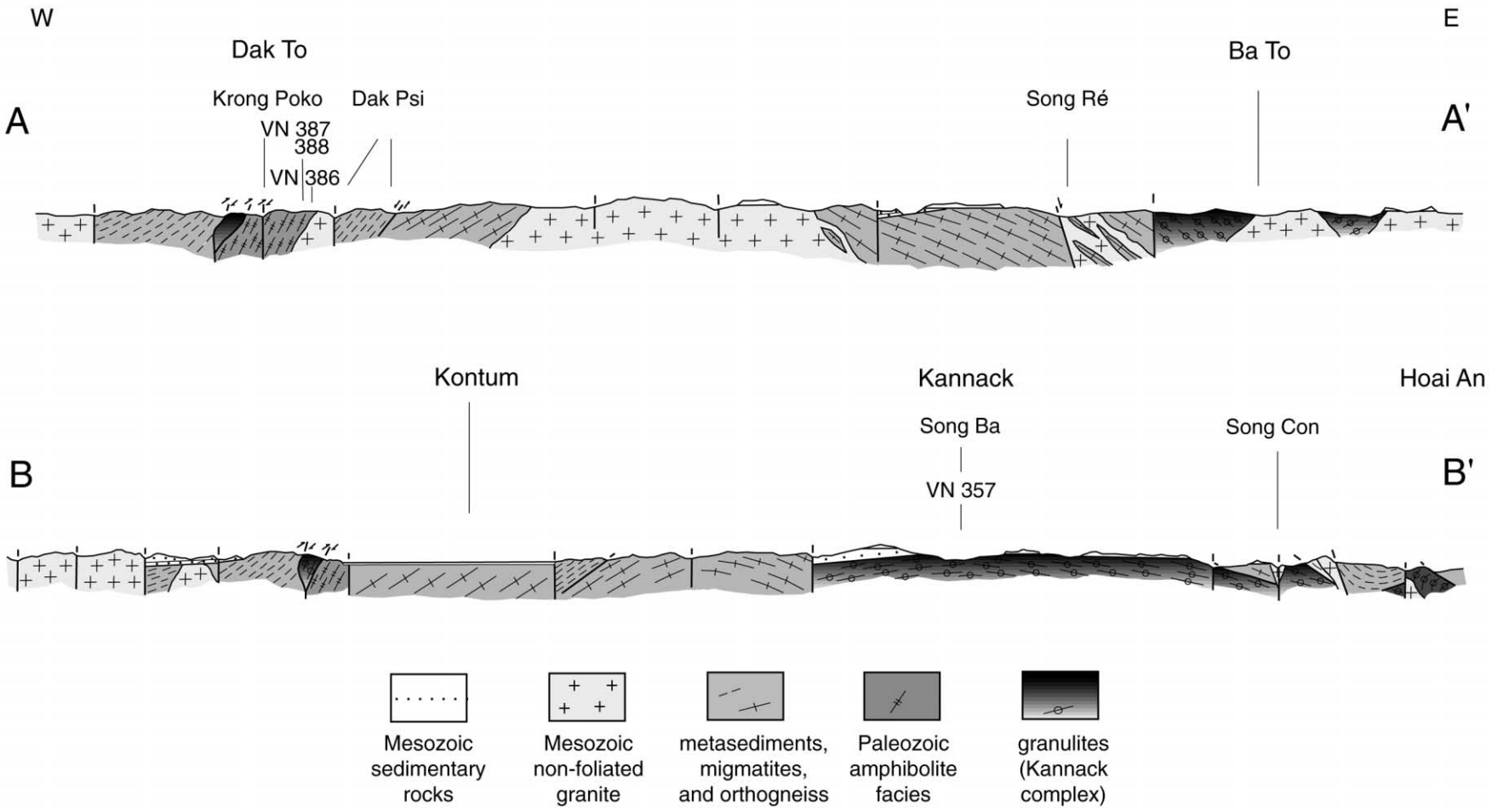

Figure 2. Geologic cross sections corresponding to *A*–*A*′ and *B*–*B*′ in figure 1 and showing Mesozoic and older rocks. The amphibolite facies rocks are shown here without the lithologic distinctions (metasediments, migmatites, orthogneiss) shown in figure 1. Elongate symbols show general direction of foliation in the various rock types. Short dashes are mica schists; other amphibolite facies units are shown with long dashes with single cross bar.

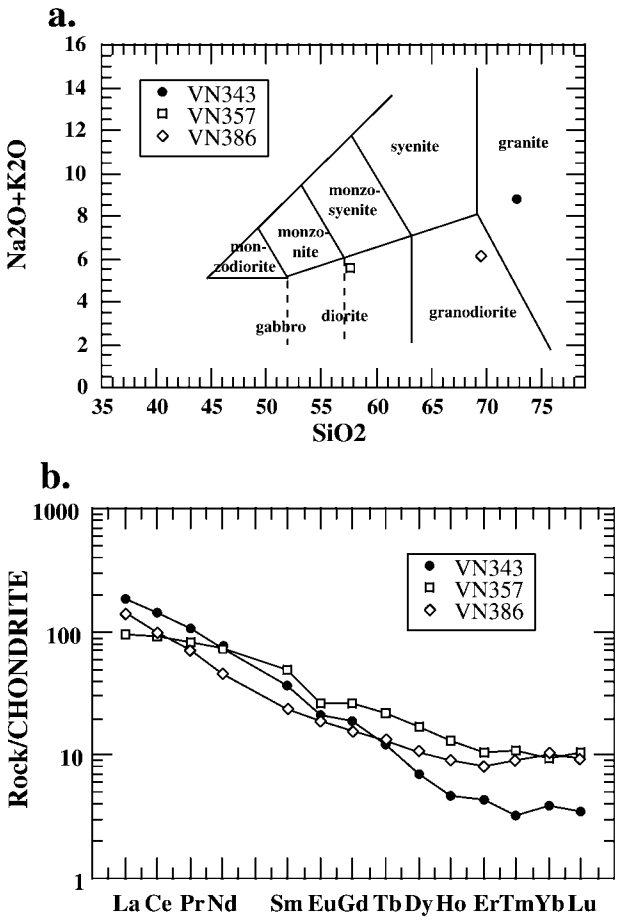

Figure 3. Geochemical results from samples VN343, VN357, and VN386 illustrated by (*a*) a total alkali-silica diagram (boundary positions after Le Bas et al. 1986) and (*b*) rare earth element patterns normalized to chondritic composition (normalizing values from Anders and Ebihara 1982).

discrimination diagrams applied to granitic rocks (Pearce et al. 1984), the granite (VN343) and granodiorite (VN386) samples generally fall within the syn-collisional and volcanic-arc granite fields, respectively.

Geochronologic Data

Previous Data. Previous studies have not quantitatively identified Archean ages for rocks from any part of the Kontum massif. Of particular significance, Archean ages inferred for the Kannack metamorphic complex in the central and eastern regions of the Kontum massif are based exclusively upon lithologic correlations inferred between the charnockites and petrologically similar Precambrian rocks in Gondwana (Phan Truong Thi 1985; Tran Quoc Hai 1986; Hutchison 1989, p. 152). K-Ar geochronology in the Kontum massif provided Early Proterozoic ages (1650–1810 Ma; Tran Quoc Hai 1986; Hutchison 1989) that are similar to, yet slightly older than, Rb-Sr ages of 1400–1600 Ma (Phan Truong Thi 1985); a 2300-Ma Pb-isochron age has also been mentioned in the literature (Hutchison 1989, p. 300). A significantly younger K-Ar biotite age of 398 ± 7 Ma has been reported from the Dak-Tô region northwest of Kontum (fig. 1; Faure and Fontaine 1969; Snelling 1969). Radiometric ages have only recently been reported directly for the Kannack complex (many of the ages reported by Hutchison [1989] are estimates) and include K-Ar ages of 241–244 Ma from synkinematic biotites in a cordierite-sillimanite-biotite gneiss (Tran Ngoc Nam 1998), a 240-Ma $^{40}Ar/^{39}Ar$ age for a charnockite (Maluski and Lepvrier 1998; Maluski et al. 1999*a*), and U-Pb SHRIMP ages around 250 Ma for a granulite (Tran Ngoc Nam et al. 2001).

U-Pb and Rb-Sr Analyses. Zircons from samples VN357, VN343, and VN386 were dated with the U-Pb technique, and K-feldspars from the samples were analyzed for Rb-Sr and Pb isotope systematics. Measurements were performed using the isotope dilution method on grain-by-grain selected fractions of zircon and K-feldspar, concentrated using conventional magnetic and density separation techniques following crushing of 3–5-kg rock samples. The U-Pb and Rb-Sr analytical results are listed in tables 2 and 3, respectively. Most grains were abraded prior to dissolution (indicated in table 2). All U-Pb dates were corrected for initial common Pb as determined on coexisting K-feldspars from each sample (table 3 [tables 1, 3, and 5 are available from *The Journal of Geology* Data Depository free of charge upon request]). Details of the analytical procedures and mass-spectrometric analysis can be found in the footnotes of tables 2 and 3 and in earlier publications (e.g., Schärer et al. 1994; Zhang and Schärer 1999).

Concordia diagrams for the diorite and granite charnockites and the amphibolite facies granodiorite are shown in figure 4*a*–4*c*, respectively. Seven zircon fractions from VN357 (fig. 4*a*) yield five concordant and two slightly discordant dates. The mean age defined by the five identically concordant zircon fractions and the very slightly discordant fractions is 248.8 ± 1.7 (2σ) Ma. A regression line including all seven fractions gives an upper intercept age of about 1.1 Ga, approximating the age of zircons from the melted crustal material. Seven zircon fractions from VN343 (fig. 4*b*) yield two concordant ages and one very slightly discordant date that together give a mean age of 252.5 ± 1.5 Ma,

Table 2. U-Pb Analytical Results for Zircons from the Kontum Region

Sample description	Mass (mg)	Concentration (ppm) U	Concentration (ppm) Pb rad.	$^{206}Pb/^{204}Pb$ measured[a]	Radiogenic Pb in atomic %[b] ^{206}Pb	^{207}Pb	^{208}Pb	Atomic ratios[b] $^{206}Pb/^{238}U$	$^{207}Pb/^{235}U$	$^{207}Pb/^{206}Pb$	Apparent ages in Ma[b] $^{206}Pb/^{238}U$	$^{207}Pb/^{235}U$	$^{207}Pb/^{206}Pb$
Dioritic charnockite (VN357):													
~45 medium to large equant grains, transparent, abraded	.1626	313	13.0	651	81.8	4.2	13.9	.03944	.2816	.051773	249	252	275
~30 large egg-shaped to elongate grains, transparent, abraded	.0984	349	14.2	514	84.3	4.3	11.4	.03996	.2810	.051009	253	251	241
~35 large elongate grains, transparent, nonabraded	.1798	383	15.6	1165	82.6	4.2	13.1	.03913	.2770	.051339	247	248	256
~7 large elongate grains, transparent, nonabraded	.0722	402	15.7	1166	85.5	4.4	10.1	.03882	.2726	.050938	245	245	238
~5 medium to large egg-shaped to round grains, transparent, strongly abraded	.0369	263	11.0	1508	80.7	4.2	15.0	.03919	.2833	.052426	248	253	304
14 medium to large broken pieces of grains, transparent, abraded	.0790	160	6.6	568	81.7	4.2	14.1	.03887	.2761	.051518	246	248	264
~15 large elongate grains, transparent, nonabraded	.1565	377	15.8	3221	83.6	4.4	12.0	.04077	.2952	.052509	258	263	308
Granitic charnockite (VN343):													
~13 large elongate grains, transparent, abraded	.0484	498	22.0	4576	77.2	4.0	18.9	.03958	.2810	.051478	250	251	262
~11 large elongate to round grains, transparent, abraded	.0251	470	21.1	1012	76.3	3.9	19.7	.03978	.2828	.051562	251	253	266
~15 medium to large egg-shaped grains, transparent, strongly abraded	.0377	513	19.9	3063	88.8	4.6	6.6	.04009	.2861	.051755	253	255	275
~10 large elongate grains, transparent, nonabraded	.0673	2183	72.7	11,349	91.5	4.7	3.9	.03543	.25014	.051206	224	227	250
~22 medium to large, round to egg-shaped grains, transparent, abraded	.1190	1521	63.6	11,498	89.2	5.7	5.1	.04341	.38073	.063616	274	328	729
~17 medium equant grains, transparent, abraded	.0496	1220	59.8	9116	88.6	5.8	5.5	.05056	.4583	.065746	318	383	798
24 small to medium egg-shaped grains, transparent, well abraded	.0360	1164	47.9	2597	88.0	4.9	7.1	.04210	.3260	.056159	266	287	459
Granodiorite (VN386):													
13 medium well-rounded grains, transparent, well abraded	.0435	620	43.8	5613	88.7	5.0	6.3	.07298	.5667	.056321	454	456	465
12 medium to large angular grains, transparent, abraded	.0608	586	41.6	317	87.8	4.9	7.3	.07238	.5539	.055502	450	448	433
26 small to medium equant grains, transparent, abraded	.0325	603	42.1	4096	89.2	5.0	5.9	.07238	.5554	.055653	450	449	439
19 small to medium egg-shaped grains, transparent, abraded	.0429	471	32.0	311	88.4	5.0	6.6	.06993	.5455	.056582	436	442	475
8 medium to large elongate grains, transparent, non-abraded	.0567	1215	74.5	7802	90.4	5.1	4.5	.06451	.4986	.056064	403	411	455
5 medium to large round grains, transparent, abraded	.0622	574	33.1	1169	89.8	4.9	5.3	.06028	.4578	.055082	377	383	416

Note. Individual analyses were performed on euhedral, unbroken, crack-free grains of highest transparency possible. Small grains are <80 mm long, medium-size grains are 80–120 mm long, and large grains are >120 mm long. Zircons were dissolved in HF > 50% at 220°C for 4 d in Teflon bombs; the chemical procedure is from Krogh (1973), and abrasion was performed according to Krogh (1982). U decay constants used are those determined by Jaffey et al. (1971) as recommended by Steiger and Jäger (1977). For isotopic measurements, Pb and U were loaded together on single Re filaments with Si gel and H_3PO_4 and were run at 1350°–1450°C and 1450°–1550°C, respectively, on a Thomson 206 solid-source mass spectrometer. Mass discrimination is 0.10% ± 0.05%/amu for Pb and U. Dioritic charnockite (VN357) mean (1–6): 248.8 ± 1.7 (2σ) Ma; granitic charnockite (VN343) mean (8–10): 252.5 ± 1.5 Ma; granodiorite (VN386) mean (15–17): 451.2 ± 2.6 Ma, mean (15–18): 448.1 ± 4.6 Ma.

[a] Ratio corrected for mass discrimination and isotopic tracer contribution.

[b] Ratio corrected for mass discrimination, isotopic tracer contribution, 10 pg of Pb blank, 1 pg of U blank, and initial common Pb (table 4) as determined in leached coexisting feldspar (Schärer 1991) from the samples. Together with mass-spectrometric precisions and uncertainties from spike calibration, such correction for initial Pb yields analytical uncertainties of 0.5%–0.7% for $^{206}Pb/^{238}U$, 0.6%–1.0% for $^{207}Pb/^{235}U$, and about 0.2%–0.5% for $^{207}Pb/^{206}Pb$, dependent on $^{206}Pb/^{204}Pb$ measured.

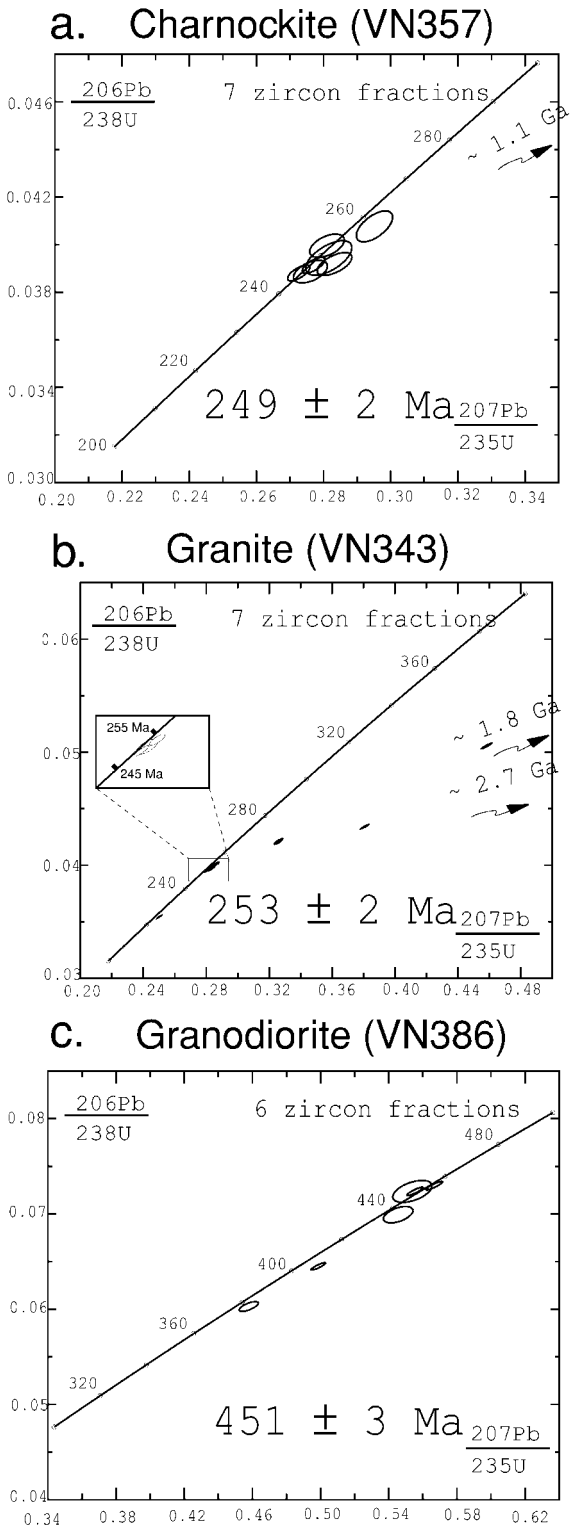

Figure 4. U-Pb concordia diagrams for samples (*a*) VN357, (*b*) VN343, and (*c*) VN386.

whereas three other fractions are significantly discordant, indicating the presence of 1.8–2.7-Ga inherited components extracted from the magma source rocks. A nonabraded fraction plots at a younger age relative to all other samples, undoubtedly due to postcrystallization Pb loss at the crystal surfaces. Six zircon fractions from VN386 (fig. 4*c*) yield three concordant dates defining a mean age of 451.2 ± 2.6 Ma, and three other fractions show various degrees of discordance that can be ascribed to postcrystallization Pb loss. Including the least discordant fraction with the concordant ones gives a mean age of 448.1 ± 4.6 Ma.

Source characteristics of the dioritic, granitic, and granodioritic magmas were examined using Rb-Sr and Pb isotopes analyzed in K-feldspar (tables 3, 4). To calculate initial $^{87}Sr/^{86}Sr$ ratios (Sr_i), we corrected for the in situ decay of ^{87}Rb using the U-Pb ages of the rocks and the measured Rb/Sr ratio. The initial Pb isotope ratios (Pb_i) were measured directly on K-feldspar mineral fractions, which are generally devoid of U. The feldspars were leached with weak HF/HBr prior to dissolution to avoid analyzing chemically altered crystal rims that potentially include U and Pb from intergranular phases.

Sr_i values for the three samples lie between 0.70939 and 0.71639 (table 4). The 253-Ma granite charnockite (VN343) shows the largest crustal contribution, which is in agreement with (1) its granitic composition, compared to the less differentiated granodioritic-dioritic compositions of the other two rocks, and (2) the presence of significant inherited components in its zircons (fig. 4*b*). The Sr_i signatures in the diorite and granodiorite indicate a less significant crustal component in their source magmas, consistent with their chemical character.

Pb_i values for all three samples are slightly higher than the model curves for Pb evolution in average or upper continental crust (α–β diagram, fig. 5*a*). Because Pb is buffered by continental components, which carry the dominant portion of Pb compared to mantle melts, a contribution of only a small percentage of upper crustal material to a basaltic magma dominates the Pb isotope composition at the time of pluton emplacement (e.g., Schärer 1991). Our samples, including the diorite, therefore plot along the model curves for continental crust but in a slightly higher position, implying assimilation of old crustal components with $^{207}Pb/^{206}Pb$ values higher than both average and upper continental crust values (Stacey and Kramers 1975; Zartman and Doe 1981). This conclusion from the Pb systematics corroborates the presence of 1.1–2.7-Ga inherited components in the zircons (fig. 4). An

Table 4. Summary of Ages and Initial Sr and U-Th-Pb Signatures

Sample	$^{40}Ar/^{39}Ar$ age (Ma), 2σ s.e.	U-Pb age (Ma), 2σ s.e.	$(^{87}Sr/^{86}Sr)_i$ of magma source	$^{238}U/^{204}Pb$ (μ) of magma source	Th/U (κ) of magma source
Dioritic charnockite (VN357)	243 ± 4	248.8 ± 1.7	.71082	9.50	3.92
Granitic charnockite (VN343)	…	252.5 ± 1.5	.71639	9.64	3.90
Granodiorite (VN386)	339 ± 8	451.2 ± 2.6	.70939	9.67	3.74
Orthogneiss (VN387)	380 ± 6	…	…	…	…
Dioritic amphibolite (VN388)	424 ± 10	…	…	…	…

Note. $(^{87}Sr/^{86}Sr)_i$ is calculated from the Rb-Sr data listed in table 3 and the U-Pb age listed above. μ and κ are calculated from the Pb data listed in table 3 and the U-Pb age listed above, using a single-stage evolution model of a 4.56-Ga-old Earth having Pb initial isotopic ratios as measured in the Canyon Diablo Fe-meteorite (Tatsumoto et al. 1973).

α–γ diagram of Pb_i (fig. 5*b*) reveals that magma sources for the charnockites (VN343, VN357) are enriched in Th relative to U (Th/U [κ]: 3.92 and 3.90; table 4). These κ ratios are higher than typical of model upper or average crust, possibly indicating assimilation of lower crust material (i.e., depleted in U). In contrast, the older granodiorite (VN386) has a κ ratio (3.74) that suggests magma contribution from typical upper crust.

$^{40}Ar/^{39}Ar$ Biotite Analyses. Four samples were irradiated with flux monitors at the Osiris Reactor (CEA) in Saclay, France. Analyses were performed by stepwise heating of purified biotite separates and measured using a modified Thomson rare gas mass spectrometer. Analytical procedures can be found in earlier publications (Maluski 1989; Maluski et al. 1995*a*; Lepvrier et al. 1997). Data are presented in table 5 (tables 1, 3, and 5 are available from *The Journal of Geology* Data Depository free of charge upon request) and illustrated in figure 6.

A plateau age of 243 ± 4 Ma (2σ) is given by the last three heating steps of charnockite VN357 (fig. 6*a*). This age accounts for about 50% of the ^{39}Ar degassed between 1050°C and the temperature of complete fusion. The age calculated for the entire data set is 239 ± 5 Ma, which overlaps with the former value given uncertainties. Ages reach the range of the plateau value by low temperatures (e.g., 242 ± 8 Ma for the 700°C step). This suggests that postcooling thermal effects were insignificant.

The three amphibolite facies samples (VN386, VN387, VN388) give very similar age spectra patterns. Their plateau ages are reached early in the step-heating procedure, generally by 650°C, and the plateaus include more than 75% of the extracted ^{39}Ar (fig. 6*b*–6*d*). Plateau ages are 339 ± 8 Ma, 380 ± 6 Ma, and 424 ± 10 Ma, respectively.

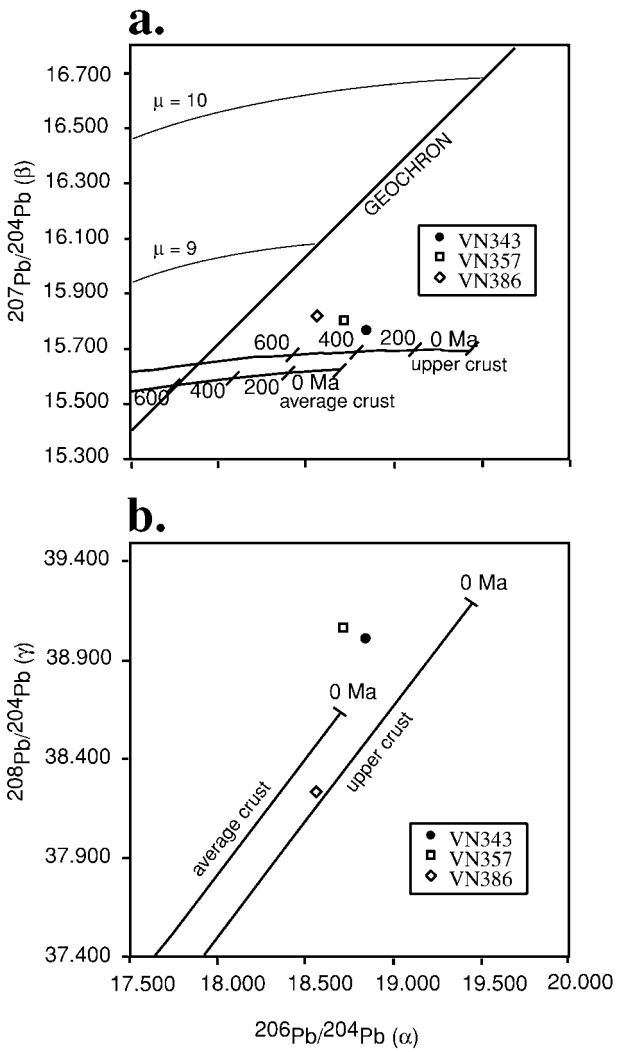

Figure 5. *a*, α–β and *b*, α–γ diagrams. Also shown are model curves for Pb-isotope evolution of upper (Zartman and Doe 1981) and average (Stacey and Kramers 1975) continental crust.

Discussion

Our geochronologic results (table 4) show that magmatism producing charnockites and amphibolite facies intrusions in the Kontum massif is much

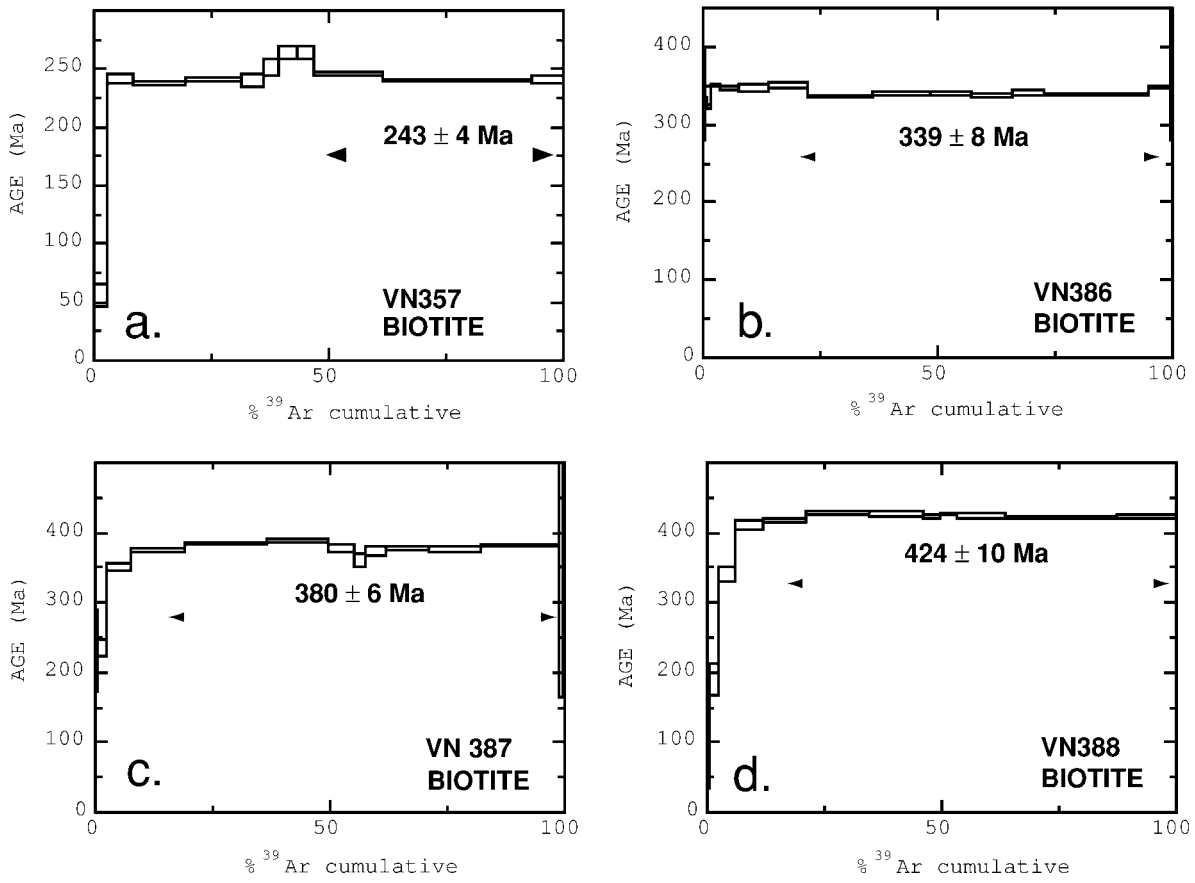

Figure 6. $^{40}Ar/^{39}Ar$ plateau diagrams for samples (*a*) VN357, (*b*) VN386, (*c*) VN387, and (*d*) VN388

younger than the Precambrian ages previously inferred (e.g., Phan Cu Tien et al. 1988; Hutchison 1989, p. 152). The Kontum massif appears to be a composite block made up of remnants of at least two magmatic events, one involving Paleozoic middle crustal plutonism and the other generating Permo-Triassic lower crustal charnockites. It follows that the Kontum massif, and in particular the Kannack metamorphic core complex, did not rift from the Precambrian granulite belt of Gondwana, which is presently dispersed in East Antarctica, India, Sri Lanka, and Australia (Katz 1993). It should, nevertheless, still be considered the principle part of the Indochina block in paleogeographic reconstructions. Following a geochronologic summary of the magmatic history of the Kontum massif as recorded in our samples and a discussion of magma source characteristics, we examine the relationship between the tectonic history of the Indochina block and magmatism recorded in the Kontum region.

Magmatic History in the Kontum Massif. The amphibolite facies granodiorite (VN386) gives a U-Pb emplacement age of ~450 Ma and an $^{40}Ar/^{39}Ar$ age of ~340 Ma. The difference in these ages may be due to slow cooling. Alternatively, the weak foliation delineated by the biotite fabric may have formed during a post-450 Ma, low-temperature tectonometamorphic event that also reset the argon systematics. Retrogressive growth of epidote (pistacite) and chlorite supports such an event. Because biotites in sample VN386 show no evidence of partial resetting of the argon system (i.e., no significantly younger $^{40}Ar/^{39}Ar$ ages at low-temperature extraction steps), we infer that such a reheating event probably occurred at ~340 Ma, completely resetting the argon isotopes in the biotite of this particular sample. This scenario is further supported by Pb loss in three slightly discordant zircon fractions in VN386 (fig. 4*c*) that intercept concordia at upper Paleozoic time.

On the basis of field relationships, and in the absence of U-Pb data, we infer that the other amphibolite facies rocks (VN387 and VN388) were em-

placed contemporaneously with VN386 at ~450 Ma. All three samples appear to be part of the same series at the outcrop level in the Krong Poko River region, and there are no tectonic or intrusive contacts between them. Samples VN387 and VN388 yield $^{40}Ar/^{39}Ar$ plateau ages of ~380 Ma and 424 Ma, respectively. Again, these ages might reflect slow cooling of Ordovician intrusions, the rate of which must have varied between the three amphibolite samples given the three different $^{40}Ar/^{39}Ar$ ages. If, however, a low-temperature thermal event did occur around 340 Ma, as suggested above, the older ages of VN387 and VN388 suggest only partial argon resetting. In contrast to VN386, the age spectra obtained from the biotites in VN387 and VN388 show evidence of Ar diffusion at low degassing temperatures, corresponding to low ages relative to the plateau ages and supporting partial resetting by a postemplacement temperature rise.

Clearly, the most surprising result from the amphibolite facies magmatic suite is the Paleozoic, rather than Precambrian, U-Pb and $^{40}Ar/^{39}Ar$ ages. Our alternative interpretation to simple cooling of Ordovician intrusions at various rates, which is that a subsequent thermal event (340 Ma or younger) reset the argon systematics to varying degrees, is speculative but certainly a viable possibility given the argon and discordant zircon results. Faure and Fontaine (1969) also suggested a low-temperature reheating event based on a Paleozoic K/Ar age (398 Ma) determined for the same granodiorite as sample VN386. We would favor an earlier age (~340 Ma) for the actual reheating event based on the observations outlined above.

The charnockite sample from the Kannack complex (VN357), previously assigned an Archean age (e.g., Phan Cu Tien et al. 1988), yields significantly younger ages of ~249 Ma (U-Pb) and ~243 Ma ($^{40}Ar/^{39}Ar$) (table 4). The convergence of ages by the two different radiometric systems implies cooling to ~250°C within ~6 Ma, indicating rapid crystallization and cooling (40°–60°C/Ma) during Permo-Triassic times. A similar U-Pb age (~253 Ma) for the charnockite sample from the southern Kontum massif (VN343) is in agreement with previously reported Permo-Triassic K/Ar (Phan Cu Tien et al. 1988) and $^{40}Ar/^{39}Ar$ (Maluski and Lepvrier 1998; Maluski et al. 1999*a*) ages from this region. Results from the two geochronometers suggest rapid exhumation of the newly generated lower crust, which is, a priori, a fundamental requirement to bring charnockitic rocks through the amphibolite and greenschist stability fields to the surface.

It is significant that the amphibolite facies samples yielding middle Paleozoic $^{40}Ar/^{39}Ar$ ages in the Krong Poko River region show no effects from the Permo-Triassic thermal event that is recorded in the nearby charnockite samples. It seems likely that there is a major, post-250-Ma structure across which the Paleozoic and Permo-Triassic rocks are juxtaposed. Given the complexity of faults shown in current geologic maps (e.g., fig. 1), it is likely that one or more such structures is present in the region.

Magma Sources. Relic inherited components in zircons from charnockite samples VN357 and VN343 show U-Pb evidence for Proterozoic, and perhaps even Archean, crustal source material present in the magma source region or assimilated during magma ascent through the lower crust. Initial Sr and Pb signatures (tables 3, 4; fig. 5) also indicate the involvement of older continental crust in the genesis of both the ~250 Ma and ~450 Ma magmas. Some older crustal material, potentially in the form of sediments, must have been present during both orogenic cycles; however, this does not imply that Precambrian crust is exposed at the surface of the Kontum complex. Although the calc-alkaline intrusions from Kontum most likely represent mixing of mantle with crustal-derived magmas, such as indicated by the Sr_i signatures and the dioritic composition of VN357, the nature of melted crust cannot be rigorously determined. Pb_i isotopic values imply that crustal source materials did not have significantly evolved signatures at the time of melting, which is compatible with magma formation within and from the lower continental crust, triggered by injection of basaltic magmas from the mantle, a generally accepted scenario for the formation of a calc-alkaline series (e.g., DePaolo et al. 1991). Evidently, this hypothesis is based on a limited data set and takes into account the tectonic context.

It is useful to distinguish whether the charnockites (VN357 and VN343) are metamorphic (e.g., dehydration products of amphibolites during granulite facies metamorphism) or igneous (e.g., melting of a fertile granulite that was dehydrated during an earlier metamorphism) because the former is inferred to occur at 700°–800°C (e.g., Hansen et al. 1987), whereas the latter can occur at temperatures as high as 1000°C (Kilpatrick and Ellis 1992). The low SiO_2 content of charnockite VN357 (58%; table 1) suggests that it may be a derivative magma of cumulates associated with magmatic charnockites, whose parental compositions are generally 62% SiO_2 (Kilpatrick and Ellis 1992), whereas the high-SiO_2 charnockite (VN343) might represent a contemporaneous fractionated magma extracted from the charnockitic parent. The relatively high abun-

dances of K_2O and LILE (larger ion lithophile elements) and low abundance of CaO in VN343 support a magmatic (C type), rather than metamorphic, charnockite source (Kilpatrick and Ellis 1992). The crystallization of biotite prior to hornblende is also characteristic of igneous charnockites (Kilpatrick and Ellis 1992). Perhaps most significantly, granulite metamorphism would not produce the necessary temperatures and pressures required to reset the U-Pb systems within the zircons to generate concordant, or nearly concordant, grains (fig. 4*a*, 4*b*).

High temperatures, such as those inferred for the emplacement of magmatic charnockites, can be attained by large volumes of basalt injection into the lower crust or by processes occurring within the basal levels of thickened crust, such as produced in major continental collision zones (Kilpatrick and Ellis 1992). This lends support to a syn-collisional magmatic origin for these rocks during a major Permo-Triassic orogenesis (discussed next).

Relationship between Magmatism and Tectonic History. The Phanerozoic tectonic history of Indochina is complicated and controversial because data from the region are rare. Numerous Paleozoic rifting events tore apart the northern margin of Gondwana, producing microcontinents that eventually collided into Asia and eradicated much of the earlier geologic record. The lack of geochronologic constraints on, and scarcity of, obducted ophiolites makes it difficult to constrain the timing of the numerous ocean-forming events and microplate separations. Most paleogeographic reconstructions, consequently, rely on the presence or absence of floral and faunal assemblages linking various continental blocks. A brief overview of the tectonic history of the Indochina block, which includes the central and southern parts of Vietnam, is provided here and shows how our geochronologic results may constrain the timing of various collisional events.

It is generally agreed that, by the early to middle Carboniferous, the Indochina and South China blocks amalgamated along the Song Ma fault zone (SMFZ in fig. 1, inset) in northern Vietnam and Yunnan (e.g., Hutchison 1989; Metcalfe 1996; Sengör and Natal'in 1996). Yin and Nie (1996, p. 473) suggest that these microplates collided in the late Triassic; however, there is significant evidence for a Carboniferous suture between the two blocks. According to Hutchison (1989), the Annamitic plutonic arc formed above a region of subduction in the late Devonian, and suturing was complete with the formation of the Truong Son fold belt (fig. 1, inset) and the emplacement of 330-Ma granites. The ages discussed by Hutchison (1989) are predominantly K-Ar determinations that the author admits need to be verified with more rigorous radiometric techniques. Additional evidence for a Late Devonian/Early Carboniferous age for the Song Ma suture zone includes middle Carboniferous carbonates that blanket the zone, different pre-middle Carboniferous faunas on either side of the zone overlain by similar middle Carboniferous faunas, and large-scale folding, thrusting, and nappe formation in the early to middle Carboniferous (Metcalfe 1998).

We have suggested that the Silurian to Carboniferous $^{40}Ar/^{39}Ar$ ages for the three amphibolite facies rocks from the Krong Poko River region in western Kontum (VN386, VN387, VN388) may reflect a low-temperature (tectonometamorphic) reheating event of Ordovician intrusions during the Early Carboniferous (340 Ma). It seems reasonable that this thermal event corresponds to a temperature increase in the crust directly related to crustal thickening and microplate collision along the Song Ma suture. If this is the case, it implies that the Kontum block, which was formerly described (e.g., Tran Van Tri et al. 1979) as an independent unit from the Truong Son fold belt north of the Tamky–Phuoc Son fault zone (fig. 1 and inset), was in fact in contact with the Truong Son belt prior to Permo-Triassic times and subsequently suffered the same temperature and deformation history.

A major Permo-Triassic collisional and suturing event between Indochina and Sibumasu (including peninsular Malaysia, Thailand, Burma, and Yunnan) closed the Paleo-Tethys Sea. We refrain from using the terms "Indosinian" or "Cimmeride" orogeny in order to avoid some controversy surrounding their appropriateness (e.g., Hutchison 1989; Sengör and Natal'in 1996), although it is clear that widespread orogenic and magmatic events occurred in Indochina during late Paleozoic/early Mesozoic times. There is general agreement that the closing of the Paleo-Tethys Sea, which produced several major N-to-NW-trending suture zones, occurred in the Triassic with orogenesis continuing into the Jurassic (e.g., Hutchison 1989; Metcalfe 1998).

A fair amount of $^{40}Ar/^{39}Ar$ and U-Pb data has confirmed the key role of this Permo-Triassic tectonometamorphic event in the NW-striking Truong Son fold belt (fig. 1) between the Song Ma suture and northern Kontum (Maluski et al. 1995*b*; Lepvrier et al. 1997; Nagy and Schärer 1999; Tran Ngoc Nam et al. 2001), as well as in the Song Chay massif (fig. 1, inset) north of the Red River fault zone (Maluski et al. 1999*a*, 1999*b*). A regional study by Lep-

vrier et al. (1997) found consistent $^{40}Ar/^{39}Ar$ plateau cooling ages on micas around 245 Ma for calc-alkaline magmatic rocks and high-grade metamorphic rocks distributed throughout NW-trending shear zones in Vietnam north of the Kontum block.

Emplacement ages determined in this study of 249 Ma (VN357) and 253 Ma (VN343) for charnockitic intrusions in the Kontum massif are in good agreement with the ages found to the north. The Permo-Triassic intrusions, thus, probably represent collision-related, batholithic-type magmatism related to the closing of the Paleo-Tethys Sea. Trace-element geochemistry of VN343 (table 1) is similar to that found in other syn-collisional granites that experienced volatile-induced enrichment in elements such as Rb and Ta (Pearce et al. 1984). The similarity between the U-Pb and $^{40}Ar/^{39}Ar$ ages for the two charnockites suggests rapid exhumation of newly generated crust, which most likely occurred during or after collision. Rapid migration of the charnockite from the magma source region may have been facilitated by preexisting inclined shear zones formed during earlier microplate collisions or even by active crustal-scale shear zones moving contemporaneously during emplacement. In a similar manner, active transcurrent shear zones were perhaps responsible for the emplacement and upward migration of a Pan-African granite-charnockite pluton in Nigeria (Ferré et al. 1997).

Our results extend to the south the known region in Indochina affected by the extensive Permo-Triassic orogeny. The tectonometamorphic event is roughly contemporaneous with closure of a large basin that formed the E-to-W-trending Qinling-Dabieshan orogenic belt between the South and North China blocks. The age of this collision in China is most likely early Triassic, possibly initiating in the latest Permian (e.g., Eide et al. 1994; Yin and Nie 1996; Rowley et al. 1997; Hacker et al. 1998); thus it appears that several microplate collisions occurred simultaneously in Asia during Permo-Triassic times.

This discussion implies above all that the Kontum massif did not rift from the Precambrian granulite belt of Gondwana. Rather, it represents a region of Paleozoic and Permo-Triassic magmatism. The Paleozoic rocks from the area around the Krong Poko River (fig. 1) were somehow protected from the thermal and deformational effects of later Permo-Triassic magma-generating orogenesis, suggesting post-250-Ma tectonic juxtaposition of these different parts of the Kontum massif. Our results from the Kontum massif question the Precambrian age assigned to other massifs in the area, such as the Chon Buri massif in Thailand and the Palin massif in Cambodia (Hutchison 1989). We have much to learn and update regarding the geology of Indochina, which has been relatively inaccessible for decades.

Conclusions

Geochronologic data from the Kannack complex in the Kontum massif, Vietnam, imply that the Archean age commonly inferred for the region is no longer supported. Instead, new $^{40}Ar/^{39}Ar$ and U-Pb ages indicate that charnockites and amphibolite facies rocks formed from Ordovician to Permo-Triassic times and thus did not rift from the Precambrian granulite belt of Gondwana. We note, however, that the presence of a crustal source bearing Precambrian material, potentially in the form of sediments, is substantiated by inherited components retained in the zircons analyzed for U-Pb. Most significantly, these results confirm the significant role of a widespread magma-generating orogeny that began in the Late Permian/Early Triassic and was the result of closing of the Paleo-Tethys Sea. The absence of thermal effects in the amphibolite facies rocks by the Permo-Triassic orogenesis implies post-250-Ma tectonic juxtaposition of these different parts of the Kontum massif.

Prior to this study, no evidence existed for a 450-Ma magmatic event in the Indochina block. The relatively low Y and Yb concentrations in VN386 are similar to concentrations found in granites formed in volcanic arc (i.e., subduction related) settings rather than in within-plate granites and ocean-ridge granites (Pearce et al. 1984). On the other hand, a rift-related origin for VN386 is supported by trace element geochemical patterns that, normalized to ocean-ridge granites, are quite similar to within-plate granites intruded into strongly attenuated crust (e.g., relatively high concentrations of K, Rb, and Th and values of Hf, Zr, and Sm close to the normalizing values; Pearce et al. 1984). The early Paleozoic history of the Indochina block is uncertain. Some authors favor Ordovician or Silurian rifting of Indochina from Gondwana (Hutchison 1989, p. 126), whereas others suggest that rifting occurred in Late Devonian times following major intracontinental extension of the northwestern Australian shelf in the Early Ordovician (Metcalfe 1996, 1998 and references therein). If the calc-alkaline Ordovician magmatism identified here was generated in a volcanic arc setting, this would not endorse early rifting scenarios. Instead, it might support a south-to-north progression of subduction-related magmatism from the Indochina

block to the South China block where ~420–435-Ma magmatism (Li et al. 1989; Li 1994; Roger et al. 2000) has been associated with a phase of granitic magmatism that occurred during a major middle Silurian ("Caledonian") collision in southeast China that produced widespread folding, metamorphism, and granitic emplacement (e.g., Hutchison 1989).

Our geochronologic results draw into question Proterozoic and earliest Phanerozoic K-Ar and Rb-Sr ages previously reported for the Kontum massif (e.g., Phan Truong Thi 1985; Tran Quoc Hai 1986; Hutchison 1989). In several of these publications, the ages are given without supporting data tables or obtainable references, and in some cases, whole rock rather than single crystal ages were determined, which can be less reliable indicators of the age of crystallization. Hurley and Fairbairn (1972) reported a relatively young Rb-Sr whole rock age (530 Ma) for a group of rocks sampled between Da Nang and the Kontum region (fig. 1, inset). Their results are questionable, however, because of the large geographic distribution of the samples, their different origin and nature, their estimated initial ratio of $^{87}Sr/^{86}Sr = 0.704$ (considerably lower than any values analytically determined here; see table 4), and the fact that many samples in their study do not fall on their reference isochron. Further geochronology is needed to show that Archean, or even Precambrian, crust exists in Indochina. Presently, only small slices of heavily overprinted Precambrian gneisses have been identified in Vietnam along the Red River fault zone (fig. 1). The generally accepted Precambrian crystallization age of the Bu Khang complex in central Vietnam has recently been shown to be Cenozoic (Jolivet et al. 1999; Nagy et al. 1999, 2000). Significantly, a recent study by Lan et al. (2000) finds Nd model ages for the Kannack complex of 2.0–1.5 Ga, arguing against Archean crustal formation.

ACKNOWLEDGMENTS

We are sincerely grateful to our Vietnamese colleagues, including Tong Dzuy Thanh, Nguyen Van Vuong, Trinh Van Long, and Nguyen Xuan Bao, for the invaluable help they have offered during many different field trips. We thank F. Bodet for rewriting data-processing programs and helpful discussions, L. de la Cruz for help with Rb-Sr analyses, and F. Roger for providing a preprint of her results from the Song Chay massif. We thank three anonymous reviewers for helpful suggestions. This work was supported by Centre National de la Recherche Scientifique-INSU through the Programme International de Coopération Scientifique "Vietnam" and partially funded by a National Science Foundation International Research Fellowship to E. A. Nagy.

REFERENCES CITED

Anders, E., and Ebihara, M. 1982. Solar-system abundances of the elements. Geochim. Cosmochim. Acta 46:2363–2380.

Bodet, F., and Schärer, U. 2000. Evolution of the SE-Asian continent from U-Pb and Hf isotopes in single grains of zircon and baddeleyite from large rivers. Geochim. Cosmochim. Acta 64:2067–2091.

DePaolo, D. J.; Linn, A. M.; and Schubert, G. 1991. The continental crustal age distribution: methods of determining mantle separation ages from Sm-Nd isotopic data and application to the southwestern United States. J. Geophys. Res. 96:2071–2088.

DGMVN (Department of Geology and Minerals of Vietnam). 1997. Geological and mineral resources map of Vietnam (1 : 200,000), Mang Den–Bong Son sheet (D-49-XIII & D-49-XIV), Hanoi.

Eide, E. A.; McWilliams, M. O.; and Liou, J. R. 1994. $^{40}Ar/^{39}Ar$ geochronology and exhumation of high-pressure to ultrahigh-pressure metamorphic rocks on east-central China. Geology 22:601–604.

Faure, C., and Fontaine, H. 1969. Géochronologie du Vietnam méridional. Arch. Geol. Vietnam (Saïgon) 12: 213.

Ferré, E.; Gleizes, G.; Djouadi, M. T.; Bouchez, J. L.; and Ugodulunwa, F. X. O. 1997. Drainage and emplacement of magmas along an inclined transcurrent shear zone: petrophysical evidence from a granite-charnockite pluton (Rahama, Nigeria). *In* Bouchez, J. L.; Hutton, D. H. W.; and Stephens, W. E., eds. Granite: from segregation of melt to emplacement fabrics. Dordrecht, Kluwer Academic, p. 253–273.

Hacker, B. R.; Ratschbacher, L.; Webb, L.; Ireland, T.; Walker, D.; and Shuwen, D. 1998. U/Pb zircon ages constrain the architecture of the ultrahigh-pressure Qingling-Dabie orogen, China. Earth Planet. Sci. Lett. 161:215–230.

Hansen, E. C.; Janardhan, A. S.; Newton, R. C.; Prame, W. K. B. N.; and Ravidra Kumar, G. R. 1987. Arrested charnockite formation in southern India and Sri Lanka. Contrib. Mineral. Petrol. 96:225–244.

Hoang, N., and Flower, M. 1998. Petrogenesis of Cenozoic basalts from Vietnam: implication for origin of "Diffuse Igneous Province." J. Petrol. 39:369–395.

Hurley, P. M., and Fairbairn, H. W. 1972. Rb-Sr ages in Vietnam: 530 m.y. event. Geol. Soc. Am. Bull. 83: 3525–3528.

Hutchison, C. S. 1989. Geological evolution of south-east Asia. Oxford, Oxford Science Publications, 368 p.

Jaffey, A. H.; Flynn, K. F.; Glendenin, L. E.; Bentley, W. C.; and Essling, A. M. 1971. Precision measurements of half-lives and specific activities of ^{235}U and ^{238}U. Phys. Rev. C4:1889–1906.

Jolivet, L.; Maluski, H.; Beyssac, O.; Goffé, B.; Lepvrier, C.; Phan Truong Thi; and Nguyen Van Vuong. 1999. Oligocene-Miocene Bu Khang extensional gneiss dome in Vietnam: geodynamic implications. Geology 27:67–70.

Katz, M. B. 1993. The Kannack complex of the Vietnam Kontum massif of the Indochina block: an exotic fragment of precambrian Gondwanaland? *In* Findlay, R. H.; Unrug, R.; Banks, M. R.; and Veevers, J. J., eds. Gondwana 8. Rotterdam, Balkema, p. 161–164.

Kilpatrick, J. A., and Ellis, D. J. 1992. C-type magmas: igneous charnockites and their extrusive equivalents. Trans. R. Soc. Edinb. Earth Sci. 83:155–164.

Krogh, T. E. 1973. A low-contamination method for hydrothermal decomposition of zircon and extractions of U and Pb for isotopic age determinations. Geochim. Cosmochim. Acta 37:485–494.

———. 1982. Improved accuracy of U-Pb zircon ages by the creation of more concordant systems using air abrasion technique. Geochim. Cosmochim. Acta 46: 637–649.

Lan, C.-Y.; Chung, S.-L.; Lo, C.-H.; Lee, H.; Wang, P.-L.; and Lee, T.-Y. 1999. The oldest rock in SE Asia: a late Archean gneissic complex from the Red River shear zone, Northern Vietnam. EOS: Trans. Am. Geophys. Union Fall Meeting, p. F1044 (abstr.).

Lan, C.-Y.; Chung, S.-L.; Lo, C.-H.; Lee, T.-Y.; and Trinh Van Long. 2000. Crustal evolution of the Indochina block: Sm-Nd isotopic evidence from the Kontum massif, central Vietnam. EOS: Trans. Am. Geophys. Union Fall Meeting, p. F1110 (abstr.).

Le Bas, M. J.; Le Maitre, R. W.; Streckeisen, A.; and Zanettin, B. 1986. A chemical classification of volcanic rocks based on the total alkali–silica diagram. J. Petrol. 27:745–750.

Lee, T.-Y.; Lo, C.-H.; Chung, S.-L.; Chen, C.-Y.; Wang, P.-L.; Lin, W.-P.; Hoang, N.; Chi, C. T.; and Yen, N. T. 1998. $^{40}Ar/^{39}Ar$ dating result of Neogene basalts in Vietnam and its tectonic implication. *In* Flower, M. F. J.; Chung, S.-L.; Lo, C.-H.; and Lee, T.-Y., eds. Mantle dynamics and plate interactions in east Asia. Am. Geophys. Union Geodyn. Ser. 27, p. 317–330.

Lepvrier, C.; Maluski, H.; Nguyen Van Vuong; Roques, D.; Axent, V.; and Rangin, C. 1997. Indosinian NW-trending shear zones within the Truong Son belt (Vietnam): $^{40}Ar/^{39}Ar$ Triassic ages and Cretaceous to Cenozoic overprints. Tectonophysics 283:105–127.

Li, X. 1994. A comprehensive U-Pb, Sm-Nd, Rb-Sr and $^{40}Ar/^{39}Ar$ geochronologic study on Guidong granodiorite, southeast China: records of multiple tectonothermal events in a single pluton. Chem. Geol. 115: 283–295.

Li, X.; Tatsumoto, M.; Premo, W. R.; and Gui, X. 1989. Age and origin of the Tanghu granite, southeast China: results from U-Pb single zircon and Nd isotopes. Geology 17:395–399.

Maluski, H. 1989. Argon 39–Argon 40 dating—principles and applications to minerals from terrestrial rocks. *In* Roth, A., and Poty, B., eds. Nuclear methods of dating. Solid Earth Sciences Library. Dordrecht, Kluwer Academic 12:325–351.

Maluski, H.; Coulon, C.; Popoff, M.; and Baudin, P. 1995*a*. $^{40}Ar/^{39}Ar$ chronology, petrology and geodynamic setting of Mesozoic to early Cenozoic magmatism from the Benue Trough, Nigeria. J. Geol. Soc. Lond. 152:311–326.

Maluski, H., and Lepvrier, C. 1998. Overprinting metamorphisms in Vietnam. EOS: Trans. Am. Geophys. Union 79:795 (abstr.).

Maluski, H.; Lepvrier, C.; Phan Truong Thi; and Nguyen Van Vuong. 1999*a*. Early Mesozoic to Cenozoic evolution of orogens in Vietnam: an Ar-Ar dating synthesis. J. Geol., DGMV, Hanoi, Ser. B, Spec. Issue 13–14:81–86.

Maluski, H.; Lepvrier, C.; Roques, D.; Nguyen Van Vuong; Phan Van Quynh; and Rangin, C. 1995*b*. ^{40}Ar-^{39}Ar ages in the Da Nang–Dai Loc plutono-metamorphic complex (central Vietnam): overprinting process of Cenozoic over Indosinian thermotectonic episodes. Workshop on Cenozoic evolution of the Indochina peninsula, Hanoi-Do Son, 65 p.

Maluski, H.; Lepvrier, C.; Ta Trong T.; and Nguyen Duc T. 1999*b*. Effect of updoming process in the Song Chay massif (Vietnam) on Ar-Ar ages. EUG 10, Strasbourg, Terra Nova 4:57 (abstr.).

Metcalfe, I. 1988. Origin and assembly of south-east Asian continental terranes. *In* Audley-Charles, M. G., and Hallam, A., eds. Gondwana and Tethys. Geol. Soc. Spec. Publ. 37:101–118.

———. 1996. Pre-Cretaceous evolution of SE Asian terranes. *In* Hall, R., and Blundell, D., eds. Tectonic evolution of Southeast Asia. Geol. Soc. Spec. Publ. 106: 97–122.

———. 1998. Palaeozoic and Mesozoic geological evolution of the SE Asian region: multidisciplinary constraints and implications for biogeography. *In* Hall, R., and Holloway, J. D., eds. Biogeography and geological evolution of SE Asia. Leiden, Backhuys, p. 25–41.

———. 1999. Gondwana dispersion and Asian accretion: an overview. *In* Metcalfe, I., ed. Gondwana dispersion and Asian accretion. IGCP 321 Final Results Volume, p. 9–28.

Nagy, E. A., and Schärer, U. 1999. The Late Permian–Early Triassic Orogeny in Indochina: precise U-Pb dating results from Vietnam. EUG 10, Strasbourg, Terra Nova 4:670 (abstr.).

Nagy, E. A.; Schärer, U.; and Minh, N. T. 1999. Early Miocene plutonism and geodynamic significance in central Vietnam: U-Pb, Rb-Sr ages, and geochemistry. Geol. Soc. Am. Meeting 31:345 (abstr.).

———. 2000. Oligo-Miocene granitic magmatism in central Vietnam and implications for continental deformation in Indochina. Terra Nova 12:67–77.

Nguyen Xuan Bao; Tran Duc Luong; and Huynh Trung. 1994. Explanatory note to the geological map of Viêt Nam on 1 : 500,000 scale. Hanoi, Geol. Surv. Vietnam.

Pearce, J. A.; Harris, B. W.; and Tindle, A. G. 1984. Trace element discrimination diagrams for the tectonic interpretation of granitic rocks. J. Petrol. 25:956–983.

Phan Cu Tien; Le Duc An; and Le Duy Bach, eds. 1988. Geology of Cambodia, Laos and Vietnam (geologic map; 1 : 1,000,000) and its explanatory note "Geology of Cambodia, Laos and Vietnam." Hanoi, Geol. Surv. Vietnam, 158 p.

Phan Truong Thi. 1985. Metamorphic complexes of the Socialist Republic of Vietnam. *In* Lee Sang Man, ed. Explanatory text of the metamorphic map of South and East Asia (1 : 10,000,000). CGMW-UNESCO, p. 90–95.

Rangin, C.; Huchon, P.; Le Pichon, X.; Bellon, H.; Lepvrier, C.; Roques, D.; Nguyen Dinh Hoe; and Phan Van Quynh. 1995. Cenozoic deformation of central and south Vietnam. Tectonophysics 251:179–196.

Roger, F.; Leloup, P. H.; Jolivet, M.; Lacassin, R.; Phan Trong Trinh; Brunel, M.; and Seward, D. 2000. Long and complex thermal history of the Song Chay metamorphic dome (northern Vietnam) by multi-system geochronology. Tectonophysics 321:449–466.

Rowley, D. B.; Xue, F.; Tucker, R. D.; Peng, Z. X.; Baker, J.; and Davis, A. 1997. Ages of ultrahigh pressure metamorphism and protolith orthogneisses from the eastern Dabie Shan: U/Pb zircon geochronology. Earth Planet. Sci. Lett. 151:191–203.

Saurin, E. 1944. Etudes géologiques sur le Centre Annam méridional (text and 1 map). Hanoi, Bull. Serv. Geol. Indoch. 27:210.

Schärer, U. 1991. Rapid continental crust formation at 1.7 Ga from a reservoir with chondritic isotope signatures, eastern Labrador. Earth Planet. Sci. Lett. 102: 110–133.

Schärer, U.; Tapponnier, P.; Lacassin, R.; Leloup, P. H.; Dalai, Z.; and Shaosheng, J. 1990. Interplate tectonics in Asia: a precise age for large-scale Miocene movement along the Ailao Shan–Red River shear zone, China. Earth Planet. Sci. Lett. 97:65–77.

Schärer, U.; Zhang, L. S.; and Tapponnier, P. 1994. Duration of strike-slip movements in large shear zones: the Red River belt, China. Earth Planet. Sci. Lett. 126: 379–397.

Sengör, A. M. C.; Altiner, D.; Cin, A.; Ustaömer, T.; and Hsü, K. J. 1988. Origin and assembly of the Tethyside orogenic collage at the expense of Gondwana Land. *In* Audley-Charles, M. G., and Hallam, A. eds. Gondwana and Tethys. Geol. Soc. Spec. Publ. 37:119–181.

Sengör, A. M. C., and Natal'in, B. A. 1996. Paleotectonics of Asia: fragments of a synthesis. *In* Yin, A., and Harrison, T. M., eds. The tectonic evolution of Asia. Cambridge, Cambridge University Press, p. 486–640.

Snelling, N. J. 1969. Isotope geology unit. London, 1968, Annu. Rep. for 1967, IGS, p.151–152.

Stacey, J. S., and Kramers, J. D. 1975. Approximation of terrestrial lead isotope evolution by a two stage model. Earth Planet. Sci. Lett. 26:207–221.

Steiger, R. H., and Jäger, E. 1977. Subcommission on geochronology: convention on the use of decay constants in geo- and cosmo-chronology. Earth Planet. Sci. Lett. 36:359–362.

Tatsumoto, M.; Knight, R. J.; and Allègre, C. J. 1973. Time differences in the formation of meteorites as determined from the ratio of lead-207 to lead-206. Science 180:1279–1283.

Tran Ngoc Nam. 1998. Thermotectonic events from Early Proterozoic to Miocene in the Indochina craton: implication of K-Ar ages in Vietnam. J. Asian Earth Sci. 16:475–484.

Tran Ngoc Nam; Sano, Y; Terada, K.; Toriumi, M.; Phan Van Quynh; and Le Tien Dung. 2001. First SHRIMP U-Pb zircon dating of granulites from the Kontum massif (Vietnam) and tectonothermal implications. J. Asian Earth Sci. 19:77–84.

Tran Quoc Hai. 1986. Precambrian stratigraphy in Indochina, geology of Kampuchea, Laos and Vietnam. Hanoi, Sci. Publisher, p. 20–30 (in Vietnamese with English abstract).

Tran Van Tri, ed. 1973, 1977. Geologic map of Vietnam (the north part) at 1 : 1,000,000, with explanatory note. Hanoi, Science and Technology Publishing House (1977 in Vietnamese, 354 p.; 1979 in English, 71 p.).

Tran Van Tri; Tran Kim Thach; and Truong Cam Bao. 1979. Geology of Vietnam (north part). Hanoi, Vietnam, Gen. Dept. Geol., Res. Inst. Geol. Miner. Res.

Yin, A., and Nie, S. 1996. A Phanerozoic palinspastic reconstruction of China and its neighboring regions. *In* Yin, A., and Harrison, T. M., eds. The tectonic evolution of Asia. Cambridge, Cambridge University Press, p. 442–485.

Zartman, R. E., and Doe, B. R. 1981. Plumbotectonics—the model. Tectonophysics 75:135–162.

Zhang, L.-S., and Schärer, U. 1999. Age and origin of magmatism along the Cenozoic Red River shear belt, China. Contrib. Mineral. Petrol. 134:67–85.